Spark-plasma-sintering (SPS) of nanostructured titanium carbonitride powders

P. Angerer[1] , L. G. Yu[2] , K. A. Khor[2], G. Korb[1], and I. Zalite[3]

[1] *ARC Seibersdorf research, Austria*
[2] *School of Mechanical and Production Engineering, Nanyang Technological University, Singapore*
[3] *Institute of Inorganic Chemistry, Riga Technical University, Latvia*

Abstract

Spark-Plasma-Sintering (SPS) compaction experiments of nanostructured titanium carbonitride powders have been performed at 1600°C and 1800°C (sintering time = 1 min). The as-received nanostructured samples have been synthesized by rapid condensation from the gas-phase (high frequency plasma). The sintering results were compared with data obtained by various conventional sintering techniques such as pressureless sintering, gas pressure sintering, and hot pressing. The phase composition and the crystallite size were investigated by X-ray diffraction (XRD). The fracture surfaces of the sintered samples were inspected by scanning electron microscopy (SEM). The experiments show that the SPS method is capable to obtain high densities (~94% of theoretical density) combined with lower grain-size quotient d/d_0 of 5.4 - 6.5.

***Keywords**:* Spark-Plasma-Sintering; Carbonitride; Grain-size; Microstructure; TiCN

1. Introduction

The general problem of obtaining fully dense nanostructured bulk materials is of essential significance in various fields of materials engineering due to their special physical parameter. The aim of this study is to investigate the sintering of additive-free nanostructured titanium carbonitride samples by means of the spark-plasma-sintering method and to compare the results with different conventional sintering techniques.

Titanium carbonitride has acquired interest due to its unique properties. Titanium carbonitride based hardmetals ("cermets") have several potential advantages compared with conventional tungsten carbide based materials e.g. the increased hardness and refractoriness [1, 2], high wear resistance high edge strength and edge sharpness [3]. The characteristics of these compounds are discussed in publications [4-7]. A review of new applications (other than cutting tools) is given by Clark and Roebuck[8]. Due to the high melting point of the titanium cabonitride phase, metal additives are needed as binders in the conventional sintering of TiCN based cermets. Additive-free titanium cabonitride based cermets can only be obtained with a sintering temperature over 2300°C[3]. In order to consolidate the additive free titanium carbonitride cermets at relatively low sintering temperature, two methods can be introduced: use of nanocrystalline titanium carbonitride (TiCN) powders instead of conventional powders and applying advanced sintering methods such as spark plasma sintering (SPS).

The initial grain size plays a critical role in the microstructure development during sintering, particularly when the grain sizes are of nanoscale [9]. Joardar et al.[10] reported the effect of nanocrystalline binder on the sintering of submicron TiCN cermets, and Zalite [11] reported the introduction of TiN nanopowder to prevent the grain growth of WC in WC-Co cermet. But there is no report on sintering pure, additive free titanium carbonitride cermet.

The spark-plasma-sintering method can be roughly compared with the conventional hot press. Additionally a pulsed electric current is applied directly to the graphite mold. This ensures the sintering of hard-to-sinter materials with a relatively lower temperature and shorter sintering time compared to other conventional sintering methods [12, 13]. The SPS method comprises three main mechanisms of action: (a) the application of uniaxial pressure, (b) the application of pulsed voltage, and (c) the resistance heating of graphite dies and sample. Nevertheless, an exact interpretation of the microscopic effect of the SPS has not been achieved. A description of this method and its related modifications including a summary of the historical developments has been given [14].

Spark plasma sintering of conventional TiCN powder was reported by Wang et al. [15]. Spark plasma sintering of nanostructured titanium nitride powder were performed by Groza et al.[16] Studies of conventional sintering of nanocrystalline titanium nitride powders were undertaken by Rabe and Wäsche[17] and Castro and Ying.[18]

2. Experimental procedure

The product Titanium Carbonitride Nanopowder (Lot 2002/1, from Plasma Ceramics Technologies Inc., Latvia) was used for the compaction experiments. This powder was synthesized by ultra-rapid condensation from the gas phase [11]. The evaporation of the raw materials was performed by means of a high frequency plasma of 5.28 MHz (generator power 65-80 kW).

The spark-plasma-sintering-experiments were performed using an SPS-1050 apparatus (Sumitomo Coal Mining, Japan). In Fig. 1 a schematic of this device is displayed. About 2 g of the noncompacted powders were loaded in a graphite die (15mm diameter) and punch unit quickly to prevent reaction. A low internal pressure (several Pa, air) was applied at the beginning of the sintering experiment. During the sintering process the pressure increases to 10-30 Pa while reaching maximal temperature, due to the heating-up of the residual air in the

chamber, and drops to several Pa again due to the further pumping by the vacuum system. The pressure applied at the punch unit reached a maximum of 20-30 MPa. The used electric current was typically 1350A at 1600°C and 1650A at 1800°C. The corresponding voltage lay between 4 and 6 V, respectively. The electric current was pulsed periodically with 14 pulses /sec (2 of 14 pulses off as a recovery time).

The temperature was measured by means of a pyrometer on the surface of the graphite die cylinder. A temperature gradient between the measured temperature and the sample could therefore occur [19]. The internal pressure was controlled by a Pirani element. All parameters were monitored during the experiment. The heating rate lay at 100°C/min, the dwelling time was 1 min.

For the conventional pressureless sintering experiments the powders were precompacted in 15 mm steel dies with an uniaxial pressure of 50 MPa by means of 2 wt.% stearic acid as a lubricant. The obtained tablets with relative green densities between 53 and 55% were sintered afterwards in an electrical furnace (Thermal Technologies Inc., USA) under nitrogen atmosphere after removing the organic matter. This furnace is equipped with molybdenum heating elements. Thereby the heating rate was approximately 20°C /min, the dwelling time 120 min, respectively.

The hot pressing experiments were performed with an inductive heated hot pressing device, (manufactured at ARC Seibersdorf research, Austria) temperature range from 1600°C to 1800°C, dwelling time 60 min and a uniaxial pressure of 30 MPa under vacuum of 1 Pa. No sintering aid was added.

The gas pressure sintering (GPS) experiments were performed using a gas pressure sintering furnace FPW 180-250-2200-2-100PS (FCT GmbH, Germany). The sintering conditions were 2100°C under 8 MPa with nitrogen protection for a dwelling time of 45 min. The preparation of the tablets was equivalent to the pressureless sintering experiments.

3. Characterization

The determination of the density of the compacted samples was performed using Archimedes method in absolute ethanol and in distilled water.

The microstructural characterisation of the fracture surface of the compacted samples was conducted by using a scanning electron microscope (SEM) DSM-950 (C.Zeiss, Germany).The micrograph of the uncompacted nanopowder was obtained with a transmission electron microscope (TEM) CM 20 (Philips, Netherlands) using an acceleration voltage of 200 kV.

The phase characterisation of the samples and the subsequent crystallite size determination with X-ray powder diffractometry (XRD) were performed using an Philips X´Pert Powder diffractometer (r = 171.9 mm, θ – 2 θ, Bragg-Brentano geometry) using Copper $K\alpha_{1,2}$ radiation at 40 kV and 40 mA. This instrument is equipped with an automatic divergence slit, a sample spinner and a scintillation counter. A receiving slit of 0.1 mm (= 0.033° 2θ) and an antiscatter slit of 4° was selected. On both sides of the sample soller slits (0.04 rad) were inserted. The measurements were performed in step-scan mode over the range 5 – 85 ° 2θ with a step size of 0.02° and a counting time of 3 s/step.
The crystallite size determination was carried out using Scherrer´s formula in the form

$$d = K \cdot \lambda / ((B-b) \cdot \cos \theta) \qquad (1)$$

where *d* denotes the average crystallite size, K is the shape factor (normally between 0.9 and 1), λ = 1.54056 Å, is the wavelength of the used radiation, B is the peak width (FWHM or integral breadth), b = 0.08 °2θ is the instrumental standard profile width, and θ denotes the diffracting angle.

For the determination of d the main titanium carbonitride diffraction peaks at 36.5°2θ (1 1 1), 42.2°2θ (2 0 0), and 61.2°2θ (2 2 0) were applied.

For the determination of the position of the sample in the solid solution series titanium carbide - titanium nitride, i.e. the C/(C+N) ratio, the diffraction peaks at 73.0°2θ (3 1 1) and 76.9°2θ (2 2 2) were used.

4. Results and discussion

Fig. 2 shows a transmission electron microscopy (TEM) micrograph of the pristine nanopowder. The cubic crystal shape of the monocrystalline particles can be clearly seen. The diameter of these particles varies between 25 and 100 nm. This value corresponds well to data obtained from powder XRD (38 nm). Yet, with the increase of crystal grain size after sintering, the inconsistency of the grain sizes obtained by XRD to those obtained by SEM micrographs is observed. An increasing crystallite size obtained by XRD corresponds with an even larger increase of the grain size obtained by SEM. This difference can be generated by a possible polycrystalline structure of the TiCN grains. For a more precise determination of the grain size the influence of the distribution of the crystallite size, the crystallite shape, and internal stress effects should also be considered. The influence of dislocations and stacking faults, which are rarely distributed homogenously and can consequently reduce the coherence length, can effectively lower the XRD-obtained crystallite size values. The work of Fultz and Howe [20] provides further elaboration on this issue.

Another complication is the chemical composition of the powder. In Fig. 3 the diffractograms of the source material and the SPS compacted samples are shown. No significant minor phases besides titanium carbonitride are present. The shape of the diffraction maxima of the non-treated powder indicates a non-homogenous chemical composition. All peaks show a “shoulder” towards the higher 2θ angle which suggests a minor amount of a more nitrogen rich phase.

For the quantification of the C/(C+N) ratio the positions of the diffraction peaks at (3 1 1) and (2 2 2) for the compounds TiN, Ti($C_{0.3}N_{0.7}$), Ti($C_{0.7}N_{0.3}$), and TiC as given in JCPDS-PDF 38-1420, PDF 42-1488, PDF 42-1489, and PDF 32-1383 were plotted in a diagram against the C/(C+N) ratio (not shown). A relation between each peak position and chemical composition was constructed by means of linear regression assuming the validity of Vegard´s law. The mean value for C/(C+N) obtained from the two reflections was determined in that way. In this calculation the influence of the oxygen (incorporated in the carbon-nitrogen position of the crystal structure of the carbonitride) on the lattice constants is omitted.

In Fig. 4 the correspondent diffractograms between 70° and 80°2θ are shown in more detail. The theoretical peak positions for pure titanium nitride and titanium carbide are additionally plotted. The original sample can be described as a main amount of carbonitride with C/(C+N) = 0.68 with secondary nitrogen-rich phase (approx. 10 - 20%) with C/(C+N) = 0.21. The chemical homogenisation due to internal diffusion during the sintering process and the gradually shift of the main composition towards higher nitrogen contents can also be seen in Fig. 4. The samples sintered at 1600°C and 1800°C display a ratio C/(C+N) of 0.62 and 0.60, respectively.

Such a direct relation between C/(C+N) and the crystallographic parameters is only justified if there is no oxygen content incorporated in the crystal lattice and if there is no significant deviation from the stoichiometric composition i.e. Ti/(C+N) = 1.

A composition of N = 7.86 wt.%, C(total) = 11.84 wt.%, C(free) = 0.78 wt.%, O = 2.08 wt.% was obtained by chemical analysis, which corresponds with a stoichiometric formula $Ti(C_{0.57}N_{0.35}O_{0.08})_{1-x}$. Hereby is x = 0.01, which is in or below the range of the accuracy of the measurement. The formula suggests that all oxygen is in the crystal structure, the real content should be less due to the significant amount of oxygen adsorbed on the surface.

The correspondent value for C/(C+N) = 0.62, which is close to the result of the crystallographic calculation.

The analytical data therefore suggest that the stoichiometric composition is closely fulfilled and that only a part of the oxygen is incorporated in the crystal lattice.

Additionally the XRD traces of the gas pressure sintered sample (GPS 2100°C) and the hot pressed sample (HP 1800°C) between 70 and 80°2θ are given in Fig. 5. The deviation from the Voigt-function is here even more prominent compared to the SPS experiments.

The $K_{\alpha 1}$-$K_{\alpha 2}$ splitting can be easily observed in Figs. 4 and 5 due to the smaller FWHM of the diffraction maxima of the sintered samples in general. This effect should be clearly separated from the influence of chemical inhomogeneity and crystallite size.

The crystallographic questions related to the titanium carbide-nitride solid solution were investigated by several authors [21-23].

Fig. 6 shows the obtained relative density as a function of the sintering temperature. Regardless of the difficulty to compare experiments of various sintering times and different temperature measurement circumstances, the SPS process shows high densities at comparatively low temperatures. The conventional sintering process is not capable to obtain high densities of this carbonitride sample even with comparatively long dwelling times (120 min). The gas pressure sintering (GPS) process should be more intensively investigated.

For the evaluation of the sinter process the dynamics of the grain growth is crucial. In Fig. 7 the relative grain (or crystallite) growth d/d_0 as obtained by XRD is plotted as a function of the relative density for several samples. Here the SPS method can be identified by a more favourable grain growth to density ratio. Table 1 gives a compilation of the compaction data.

A significant difference between the various sintering methods can also be determined looking at the fracture surface.

The SPS compacted samples (SEM micrographs in Figs. 8 and 9) show a complete recrystallized texture with grains of various diameters between 0.3 and 5 µm with a relative homogenous distribution around 1 µm. The few larger grains are possibly generated by initial agglomerates in the source powder. The titanium carbonitride sample was filled in the graphite die before the sinter experiment without any de-agglomeration treatment as ultrasonic conditioning or mixing under liquid phase. On the other hand the GPS compacted sample show a complete different fracture surface (Fig. 10). The completely restructured surface with a coarse structure has a glassy appearance. Only a very small amount of agglomerates with a grain less than 1 µm size are observed here.

In Fig. 11 the fracture surface of a sample compacted by conventional hot pressing is shown (SEM). In this experiment no full densification has been achieved. The surface is determined by a fine grain size with pristine structure. Micrographs with higher magnification show the close relationship to the uncompacted powder samples.

The chemical composition of the carbonitride is important for the sintering behaviour of the material. Therefore the further investigation of samples with various C/(C+N) is desired. Additionally the chemical composition of the compacted samples would also be of interest due to the uncertainty of the situation of the oxygen in the samples and a possible minor change of the stoichiometric composition during the sintering process.

5. Conclusions

SPS compaction of nano-structured titanium carbonitride (TiC_xN_{1-x}) powders had been performed. The results were compared to the results obtained with various conventional sintering methods such as pressureless sintering, gas pressure sintering (GPS) and hot pressing. It showed that SPS samples achieved over 95% density over the temperature range 1600 -1800°C with a soaking time of 1 min at the pre-set temperature, which is significantly

higher than that obtained by pressureless sintering and hot pressing. GPS samples achieved comparable density (~ 95%), but the sintering temperature was much higher at 2100°C with a soaking time of 45 minutes. Further more, the grain size of the GPS sample was approximately 3 times the grain size of SPS sample.

Acknowledgement

The authors wish to thank C. Lengauer for illuminative scientific discussion concerning the topic of X-ray diffraction, and W. Costin (SEM), and M. Brabetz (TEM) for their relevant technical support.

References

1. Mari, D., Bolognini, S., Feusier, G., Cutard, T., Verdon, C., Viatte, T. and Benoit, W.: TiMoCN based cermets Part I. Morphology and phase composition. *Int. J. of Refractory Metals & Hard Materials*, 2003, 21, 37-46.

2. Mari, D., Bolognini, S., Feusier, G., Cutard, T., Viatte, T. and Benoit, W.: TiMoCN based cermets Part II. Microstructure and room temperature mechanical properties. *Int. J. of Refractory Metals & Hard Materials*, 2003, 21, 47-53.

3. Chen, L. M., Lengauer, W. and Dreyer, K.: Advances in modern nitrogen-containing hardmetals and cermets. *Int. J. of Refractory Metals & Hard Materials* 2000, 18, 153-161

4. Ettmayer, P. and Lengauer, W. The story of cermets. *Powder Metall Int* 1989, 21, 37-8.

5. Pastor, H.: Titanium-carbonitride-based hard alloys for cutting tools. *Mater Sci Eng A* 1988, 105/106, 401-9.

6. Ettmayer, P., Kolaska, H. and Dreyer, K.: Effect of the sintering atmosphere on the properties of cermets. *Powder Metall Int* 1991, 23, 224-9.

7. Ettmayer, P., Kolaska, H., Lengauer, W., & Dreyer, K., Ti(C,N) Cermets – Metallurgy and Properties, *Int. J. of Refractory Metals & Hard Materials*, 1995, 13, 343-351.

8. Clark, E. B. & Roebuck, B., Extending the application areas for titanium carbonitride cermets. *Int. J. Refractory Metals & Hard Mat.*, 1992, 11 23-33.

9. German, R. M.: *Sintering Theory and Practice*. John Wiley and Sons, Inc.New York, 1996.

10. Joardar, J., Kim, S. W. and Kang, S.: Effect of nanocrystalline binder on the microstructure and mechanical properties of ultrafine Ti(CN) cermets. *Materials Science and Engineering A*, 2003, A360, 385-389.

11. Zalite, I., Ordanyan, S., and Korb, G., Synthesis of transition metal nitride/carbonitride nanopowders and their application for modification of structure of hardmetals, 2003, *Powder Metallurgy*, 46, 143-147.

12. Khor, K. A., Yu, L. G., Chan, S. H. and Chen, X. J.: Densification of plasma sprayed YSZ electrolytes by spark plasma sintering (SPS). *Journal of the European Ceramic Society* 2003, 23, 1855–1863.

13. Khor, K. A. Cheng, K. H., Yu, L. G. and Boey, F.: Thermal conductivity and dielectric constant of spark plasma sintered aluminum nitride. *Materials Science and Engineering A,* A347, 300-305

14. Groza, J. R. & Zavaliangos, A., Sintering activation by external electrical field, 2000, *Mater. Sci. and Eng. A* 287, 171-177.

15. Wang, W., Qi, L. H., Pan, W., Liu, D. P. and Miao, H. Z.: The fabrication of TiCN-based functionally graded cermets by spark plasma sintering. *Functionally Graded Materials VII, Materials Science Forum*. 2003, 423-4, 213-218.

16. Groza, J. R., Curtis, J. D., & Krämer, M., Field-Assisted sintering of Nanocrystalline Titanium Nitride. *J. Amer. Ceram. Soc.,* 2000, 83, 1281-1283.

17. Rabe, T. & Wäsche, R., Sintering Behaviour of nanocrystalline Titanium Nitride Powders. *Nanostructured Materials*, 1995, 6, 357-360

18. Castro, D. T. & Ying, J. Y., Synthesis and sintering of nanocrystalline titanium nitride. *Nanostructured Materials*, 1997, 9, 67-70.

19. Kamiya, A., Observation of sample sintering temperature by the plasma activated sintering (PAS) furnace. *J. Mater. Sci. Lett.*, 1998, 17, 49-51.

20. Fultz, B. & Howe, J. M., Transmission Electron Microscopy and Diffractometry of Materials, 2001, (Springer-Verlag, Heidelberg).

21. Vil´k, Y. N. & Danisina, I. N., Structural parameters, X-ray and pycnometric densities of titanium carbonitride within a homogeneity region. *Poroshkovaya Metallurgiya*,1977, 12, 42-48.

22. Mitrofanov, B. V., Zainulin, Y. G., Alyamovskii, S. I., Shveikin, G. P., Homogeneity region, degree of filling, and concentration dependence of cubic titanium carbonitride lattice spacings. *Neorganicheskie Materialy*, 1974, 10, 745-747.

23. Guilemany, J. M., Sanchiz, I., & Alcobé , X., X-Ray Diffraction Analysis of Titanium Carbonitride 30/70 and 70/30 Solid Solutions. *Powder Diffraction*, 1992, 7(1), 34-35.

List of Tables

List of Figures

material	technique	T / °C	t / min	ρ / g·cm^{-3}	ρ_{rel} / %	d / nm	d /d_0
PCT 1 Ti(C,N)	SPS	1600	1	4.78	94	205	5.4
PCT 1 Ti(C,N)	SPS	1800	1	4.76	93	246	6.5
PCT 1 Ti(C,N)	GPS	2100	45	4.76	93	616	16.2
PCT 1 Ti(C,N)	HP	1600	60	4.26	84		
PCT 1 Ti(C,N)	HP	1700	60	4.38	86		
PCT 1 Ti(C,N)	HP	1800	60	4.44	87	205	5.4
PCT 1 Ti(C,N)	conv.	1500	120	3.16	62		
PCT 1 Ti(C,N)	conv.	1600	120	3.22	63		
PCT 1 Ti(C,N)	conv.	1650	120	3.35	66	64	1.7
PCT 1 Ti(C,N)	source	-	-	-	-	38	1

T = sintering temperature, t = dwell time at maximal temperature, ρ = density of the compacted sample, ρ_{rel} = corresponding relative density, d = crystallite size obtained by X-ray diffraction, d /d_0 = relative grain growth, technique = corresponding compaction method (SPS = spark plasma sintering, GPS = gas pressure sintering under 8 MPa N_2, HP hot pressing 30 MPa uniaxial pressure, conv. = conventional pressureless sintering under N_2).

Table 1

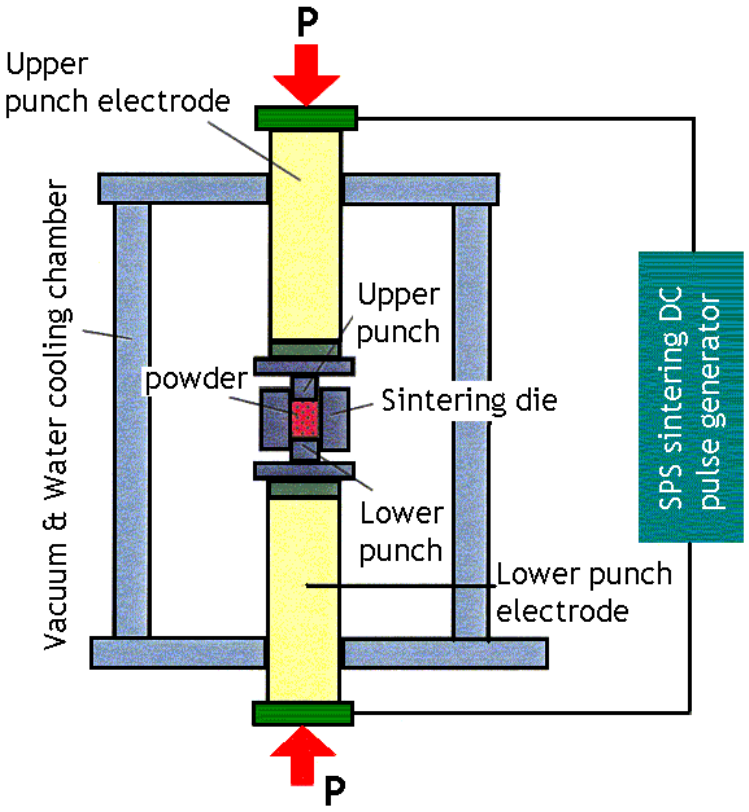
P
Upper
punch electrode
Vacuum & Water cooling chamber
Upper
punch
powder
Sintering die
Lower
punch
Lower punch
electrode
SPS sintering DC
pulse generator
P

Fig. 1

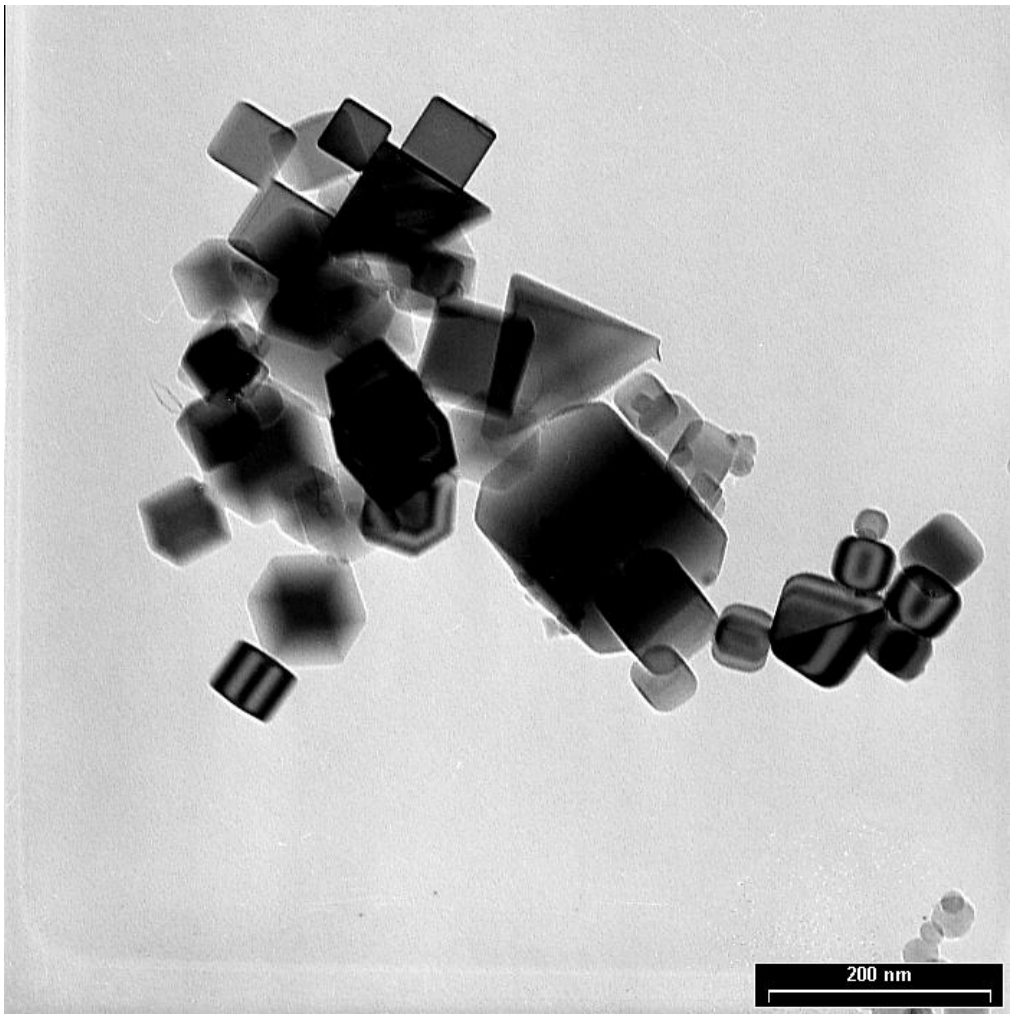

Fig. 2

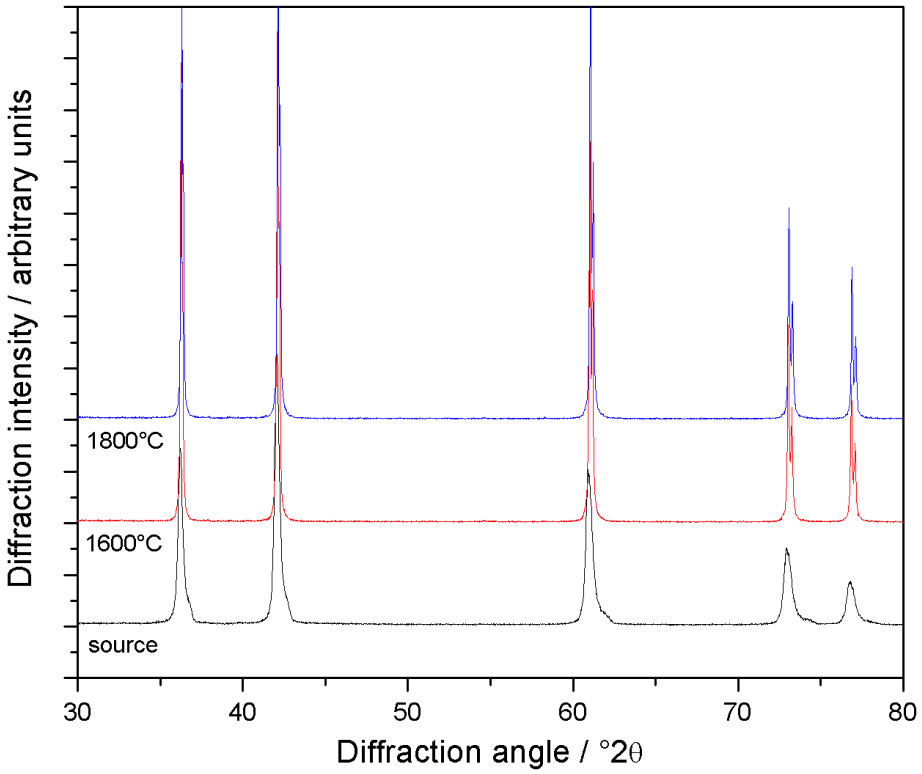
Diffraction intensity / arbitrary units
1800°C
1600°C
source
30
40
50
60
70
80
Diffraction angle / °2θ

Fig. 3

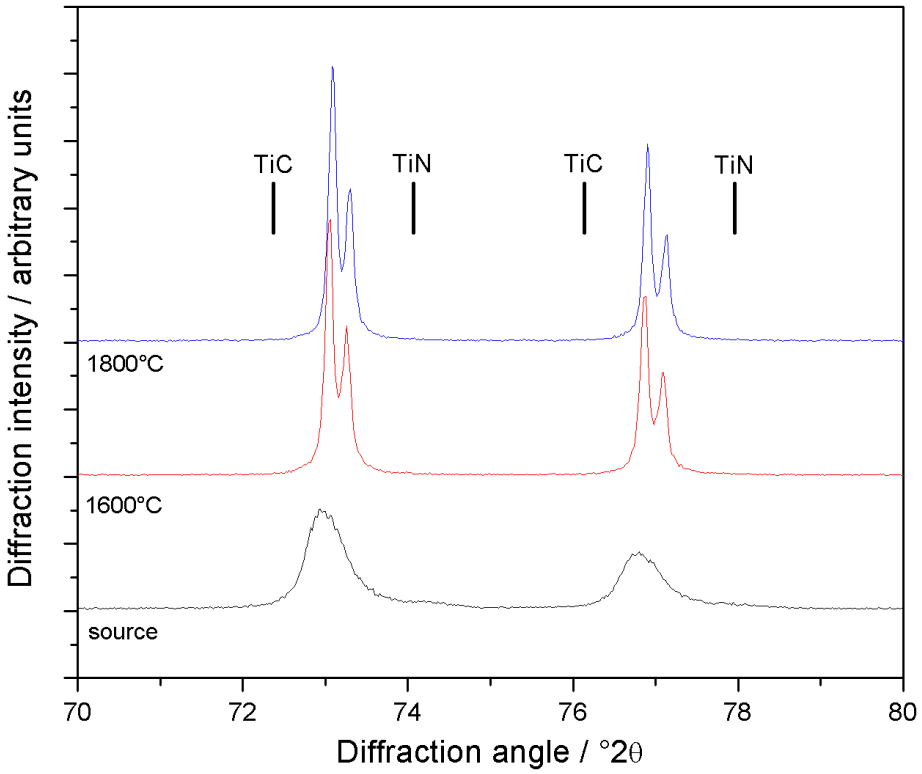
TiC
TiN
TiC
TiN
1800°C
1600°C
source
Diffraction intensity / arbitrary units
70
72
74
76
78
80
Diffraction angle / °2θ

Fig. 4

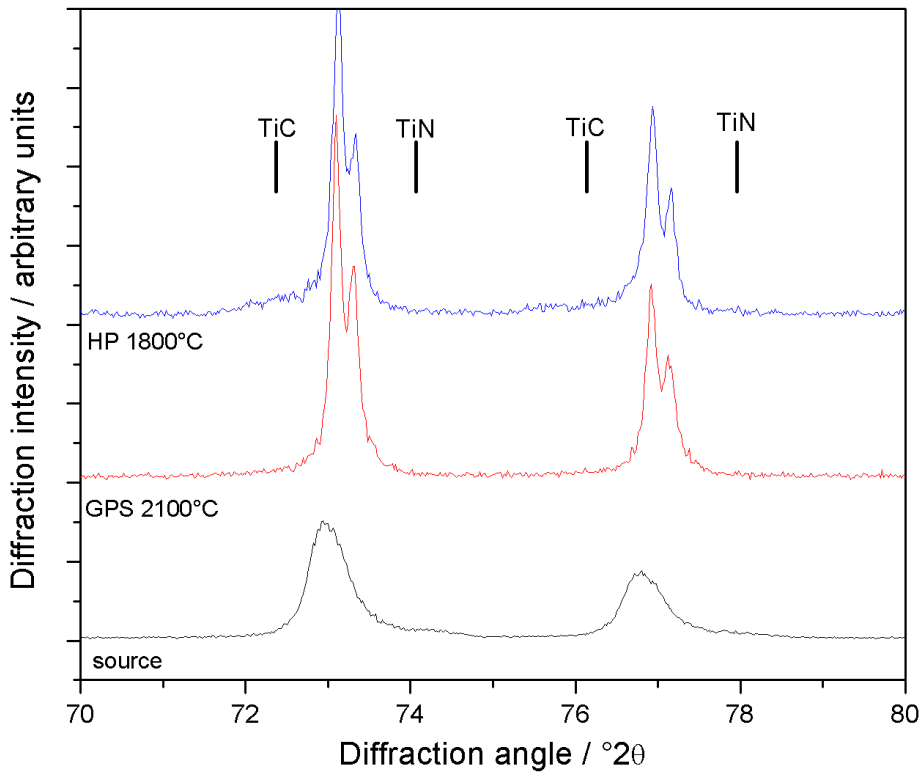
TiC
TiN
TiC
TiN
HP 1800°C
GPS 2100°C
source
Diffraction intensity / arbitrary units
70
72
74
76
78
80
Diffraction angle / °2θ

Fig. 5

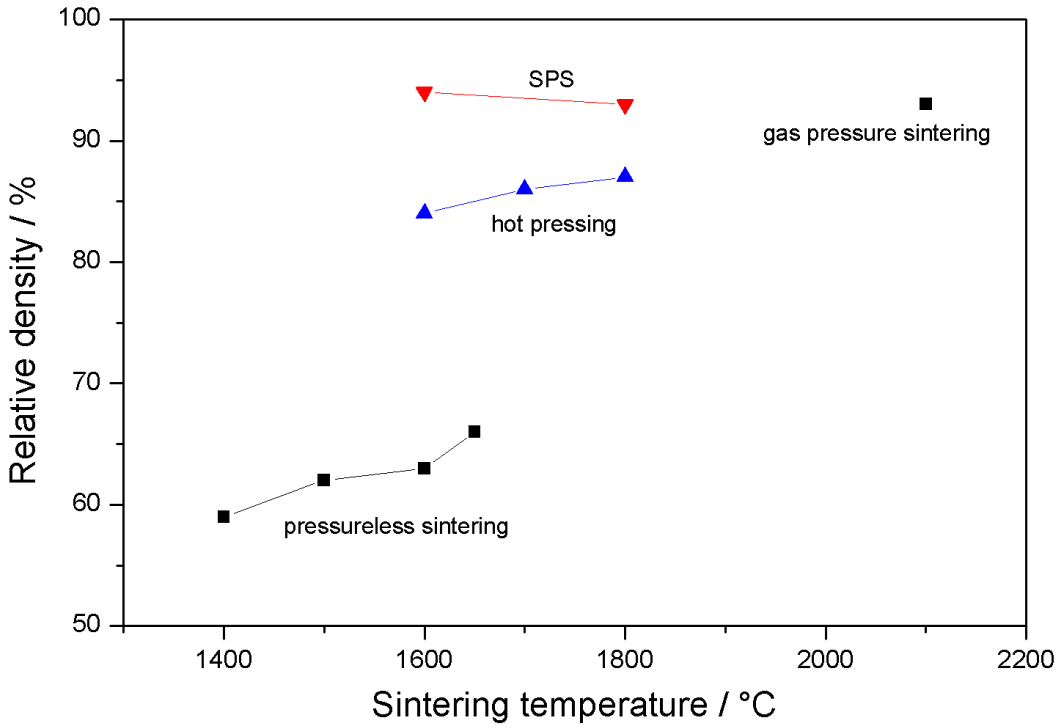
100
90
80
70
60
50
Relative density / %
1400
1600
1800
2000
2200
Sintering temperature / °C
SPS
hot pressing
gas pressure sintering
pressureless sintering

Fig. 6

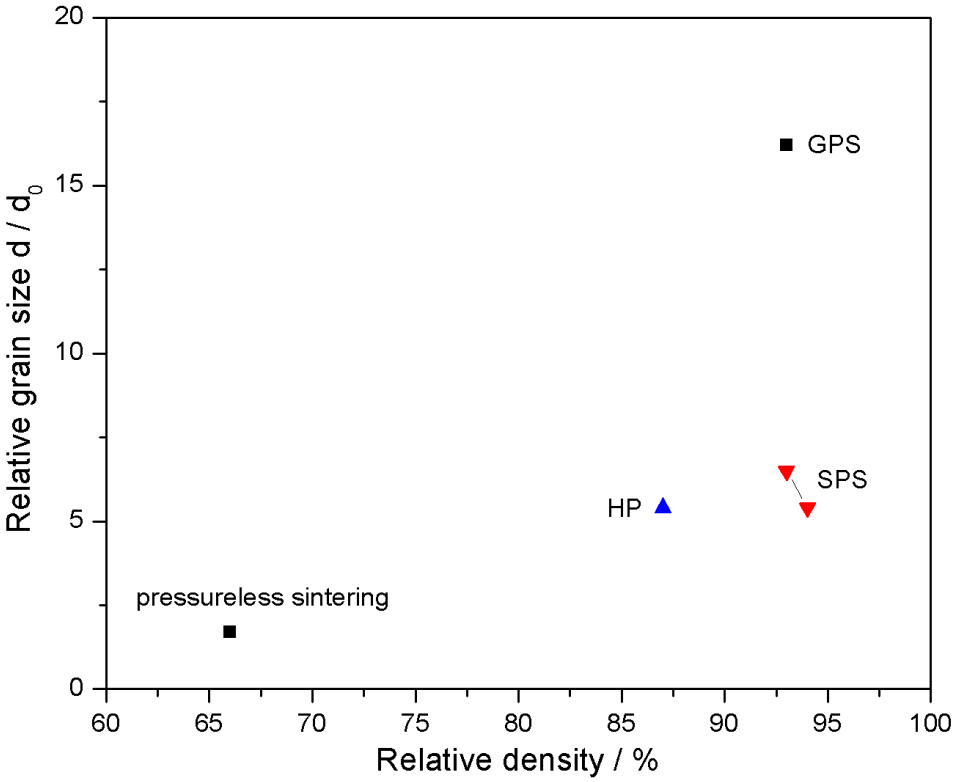
Relative grain size d / d0
Relative density / %
GPS
SPS
HP
pressureless sintering
0
5
10
15
20
60
65
70
75
80
85
90
95
100

Fig. 7:

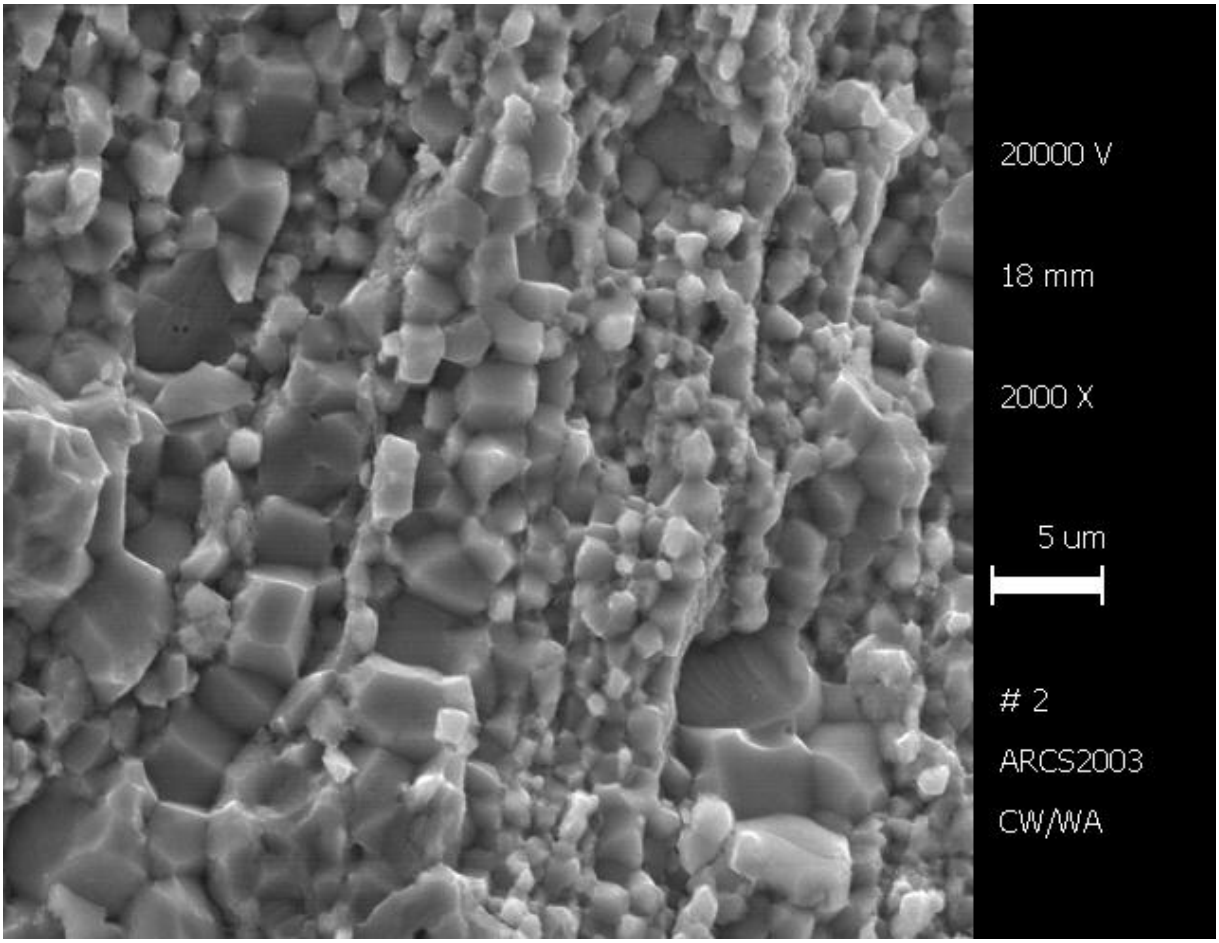

Fig. 8

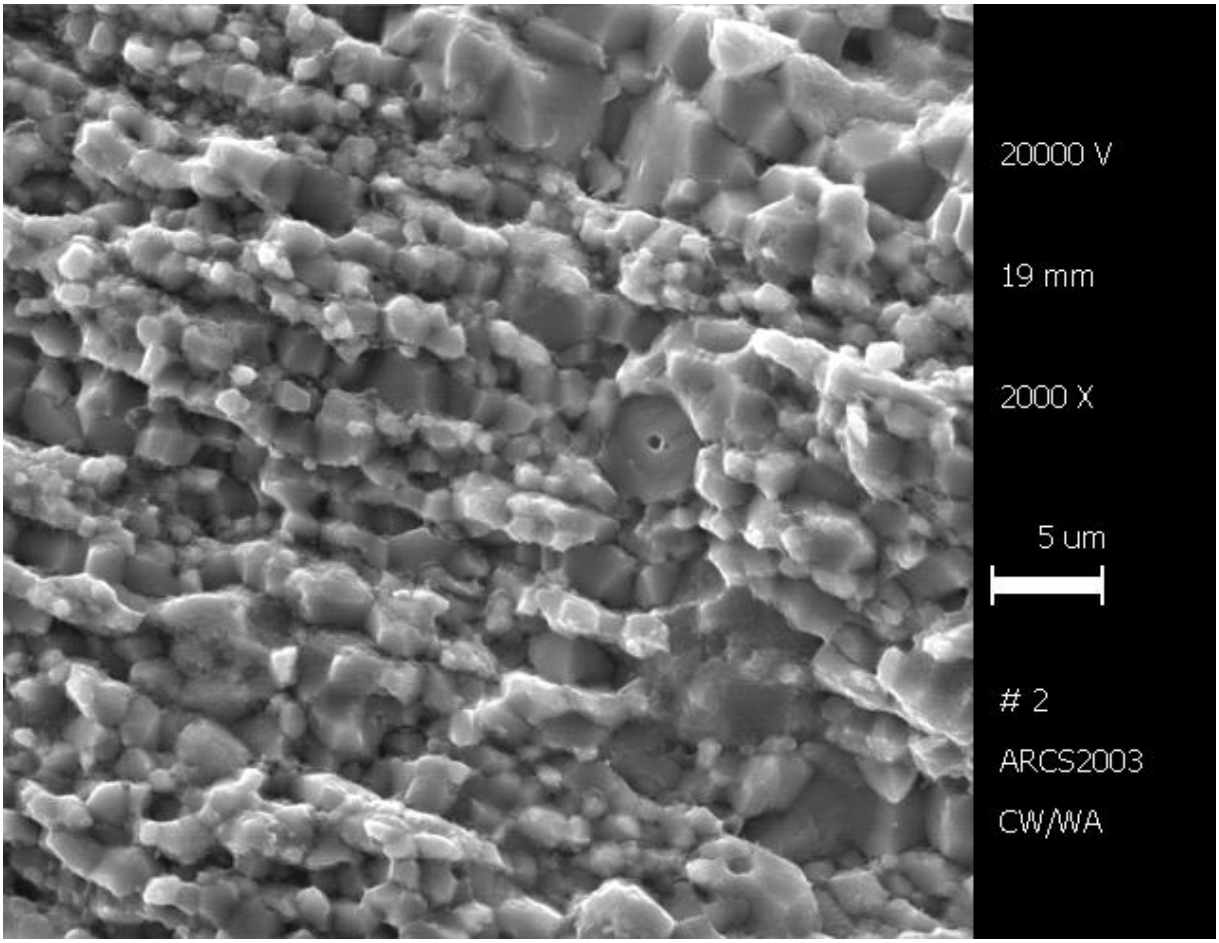

Fig. 9

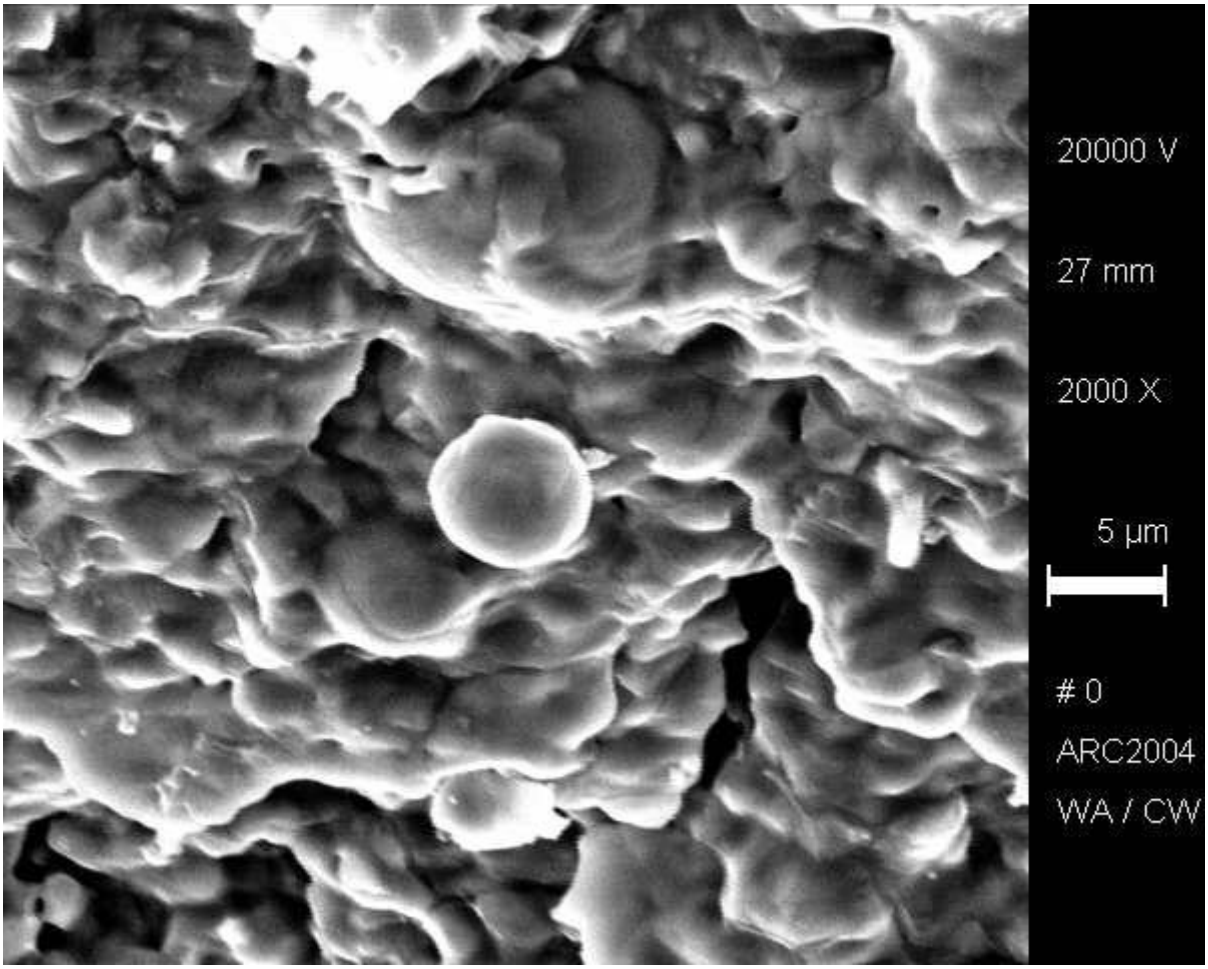

Fig. 10

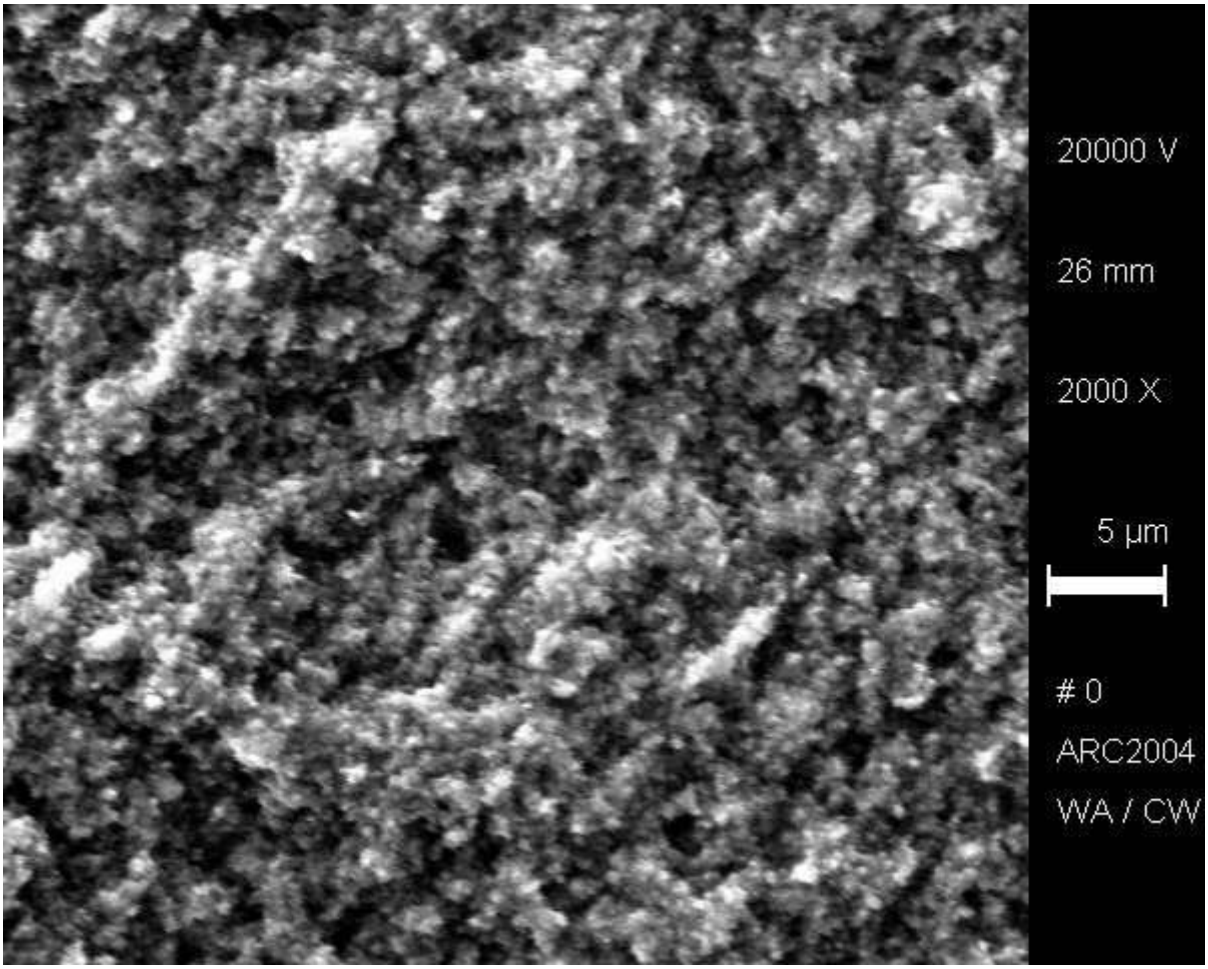

Fig. 11